Letter

# Towards high photon density for Compton scattering by spectral chirp

M. A. Valialshchikov [1,*] D. Seipt [2,3] V. Yu. Kharin [4] and S. G. Rykovanov [1,†]

[1]*Skolkovo Institute of Science and Technology, Moscow 143026, Russia*
[2]*Helmholtz Institute Jena, Fröbelstieg 3, 07743 Jena, Germany*
[3]*GSI Helmholtzzentrum für Schwerionenforschung GmbH, Planckstrasse 1, 64291 Darmstadt, Germany*
[4]*Sechenov First Moscow State Medical University (Sechenov University), Moscow 119435, Russia*

Scattering of intense laser pulses on high-energy electron beams allows one to produce a large number of x and $\gamma$ rays. For temporally pulsed lasers, the resulting spectra are broadband which severely limits practical applications. One could use linearly chirped laser pulses to compensate for that broadening. We show for laser pulses chirped in the spectral domain that there is the optimal chirp parameter at which the spectra have the brightest peak. Additionally, we use catastrophe theory to analytically find this optimal chirp value.

The scattering of intense laser pulses on high-energy electron beams is a well-established method for generating x and $\gamma$ radiation with applications in medicine, ultrafast radiography, and nuclear physics [1–6]. Recent developments in both compact powerful laser systems and compact laser-plasma-based accelerators (LPAs) [6–11] have increased interest in compact Compton photon sources. Small intensities of an incident laser pulse lead to meager photon yields. Increasing laser intensity helps to boost photon yields, but also brings nonlinear effects into play, i.e., the spectrum is redshifted and high harmonics are generated. For temporally pulsed lasers, it also leads to a significant spectral ponderomotive broadening [12–16], which severely limits practical applications of such source. As a result, a lot of research was done to search for methods to compensate for or avoid such ponderomotive broadening. For example, it was proposed to use laser pulses with flat-top profiles [12] or laser pulse chirping when laser frequency is a nonlinear function of time following the change of laser pulse envelope [14,17–19]. Recently, it was shown that it is enough to use only linear chirp to significantly reduce ponderomotive broadening [20,21] and sawtooth (doubly linear) chirping also compensates the broadening quite well [22]. Moreover, it was proposed to use laser pulses with time-varying polarization to produce narrowband harmonics in Compton spectra [23,24]. Recently, it was demonstrated that one could use catastrophe theory to analytically study the photon yield enhancement for the case of a laser pulse linearly chirped in the time domain [20]. However, such laser pulses are quite challenging to realize experimentally. Alternative approaches to produce x rays with low bandwidth include using a traveling-wave setup that allows the overlap of laser and electron beams much longer than Rayleigh length [25,26] or, instead of modifying the laser pulse, introduce an additional laser beam copropagating with the electron bunch [27].

In this Letter, using catastrophe theory and numerical simulations, we show that using linearly chirped laser pulses in the spectral domain significantly increases the peak photon number compared to the nonchirped nonlinear Compton spectrum. Additionally, we determine analytically the location of the optimal chirp parameter at which the photon peak is the highest. Throughout the Letter, we use natural units $\hbar = c = 1$, while the space-time and energy variables are rescaled by the incident laser frequency $\omega_0 : x\omega_0 \to x$, $\omega/\omega_0 \to \omega$. The dimensionless laser pulse amplitude is given by $a_0 = eA/m$, where $e, m$ are the absolute value of the electron charge and electron mass, respectively. Also, for calculations, we use the classical framework since for the parameters of interest the quantum parameter for head-on collision $\chi = 2a_0\gamma\omega_0/m \ll 1$, where $\gamma$ is the electron gamma factor, and a classical description is sufficient.

In the previous work [20], a laser pulse chirped in the time domain was considered. To move closer to more realistic experimental scenarios, here we consider optimized chirping in the spectral domain. The laser pulses are modeled as follows:

$$\tilde{A}(\omega) = \sqrt{2\pi} a_0 \tau \exp\left[-\frac{\tau^2}{2}(\omega - \omega_0)^2(1 - i\beta)\right], \quad (1)$$

where $\tau$ is the Fourier-limited pulse duration (i.e., with vanishing spectral phase), and second-order spectral phase parameter $\beta$ controls the amount of linear chirp.

Such a laser pulse has constant spectrum $|\tilde{A}(\omega)|^2$ for different chirp parameters. After performing the Fourier transformation, one could see that the amplitude and duration of a chirped laser pulse in the time domain depends on parameter $\beta$,

$$A(\phi) = a_{\text{eff}} \exp\left(-\frac{\phi^2}{2\tau_{\text{eff}}^2}\right) \exp\left[i\left(\phi + \frac{\beta\phi^2}{2\tau_{\text{eff}}^2} + \phi_0\right)\right],$$

$$a_{\text{eff}} = \frac{a_0}{(1+\beta^2)^{1/4}}, \ \tau_{\text{eff}} = \tau\sqrt{1+\beta^2}, \ \omega_L(\phi) = 1 + \frac{\beta\phi}{\tau_{\text{eff}}^2},$$

$$(2)$$

where $\phi_0$ is a constant phase shift that depends on $\beta$.

*maksim.valialshchikov@skoltech.ru
†s.rykovanov@skoltech.ru

We work in the frame of reference where an electron was initially at rest, $p = (m, 0, 0, 0)$, and results in the laboratory frame are obtained via Lorentz transformation to the frame where the electron was initially counterpropagating the laser pulse moving in the $+z$ direction.

The radiation emitted by an electron is given by the scattering integral [28],

$$\frac{d^2 I}{d\omega d\Omega} = \kappa \frac{\omega^2}{4\pi^2} \left| \int_{-\infty}^{\infty} d\phi \; \mathbf{n} \times [\mathbf{n} \times \mathbf{u}] \, e^{i\omega(\phi + z - \mathbf{n} \cdot \mathbf{r})} \right|^2, \quad (3)$$

where $\kappa = e^2 \omega_0$, $\mathbf{n}$ is the direction of observation, and $\mathbf{u}, \mathbf{r}$ are the vector part of the electron's 4-velocity and coordinate, respectively. We will denote the expression under the modulus by $M$ : $\frac{d^2 I}{d\omega d\Omega} = \kappa \frac{\omega^2}{4\pi^2} |M|^2$. The number of emitted photons is calculated by $\frac{d^2 N_{ph}}{d\omega d\Omega} = \alpha \frac{\omega}{4\pi^2} |M|^2$, where $\alpha$ is the fine-structure constant.

To transform the nonlinear oscillating parts in the exponent into a sum over harmonics, we use the Jacobi-Anger expansion. After the transformation for a slowly varying laser pulse envelope, one could obtain the following expression:

$$M = \sum_{n=1}^{+\infty} \int_{-\infty}^{\infty} d\phi \, B_n(\phi; \omega, \beta)$$
$$\times \exp \left[ i \int_0^\phi \omega + \omega(1 - \cos\theta) \frac{\mathbf{a}^2(\xi)}{4} - n\omega_L(\xi) d\xi \right], \quad (4)$$

where $\mathbf{A}(\phi) = [a_x(\phi) \cos\psi_L(\phi), a_y(\phi) \sin\psi_L(\phi), 0]$, $\psi_L(\phi) = \int_0^\phi \omega_L(\xi) d\xi$, $\mathbf{a}(\phi) = [a_x(\phi), a_y(\phi), 0]$, $\theta$ is the scattering angle, and $n$ is the harmonic number.

If the amplitudes $B$ are slowly varying functions of $\phi$, we could use the stationary phase approximation to estimate the values of the integrals (4). The stationarity condition determines the so-called ray surfaces in the parameter space $(\omega, \theta, \phi)$ for the $n$th harmonic,

$$\Phi'(\phi) = \omega + \omega(1 - \cos\theta) \frac{\mathbf{a}^2(\phi)}{4} - n\omega_L(\phi) = 0. \quad (5)$$

Ray surfaces from Eq. (5) in the parameter space $(k_x, k_z, \phi) = (\omega \sin\theta, \omega \cos\theta, \phi)$ for a fixed value of $\phi$ determine a set of ellipses in the $(k_x, k_z)$ plane for each harmonic [20]. The conditions for fold and cusp singularity (i.e., higher-order stationarity) are given by $\Phi''(\phi) = \Phi'''(\phi) = 0$,

$$\omega(1 - \cos\theta) \frac{(\mathbf{a}^2)'(\phi)}{4} = n\omega_L'(\phi), \quad (6)$$

$$(\mathbf{a}^2)'' = 0. \quad (7)$$

From Eqs. (5) and (6), we obtain expressions for scattered frequency and folds location,

$$\omega(\phi, \theta) = \frac{n\omega_L(\phi)}{1 + (1 - \cos\theta)\mathbf{a}^2(\phi)/4}, \quad (8)$$

$$\cos\theta(\phi) = 1 - \frac{4\beta}{\omega_L(\phi)[\mathbf{a}^2]'(\phi)\tau_{\text{eff}}^2 - \beta\mathbf{a}^2(\phi)}. \quad (9)$$

Equation (8) follows from the stationary phase condition and determines just the regular relation between frequency and

angle for a chirped pulse. Equation (9) follows from the fold condition (6) where, for frequency $\omega$, we used relation (8). For a fixed value of $\phi$, Eqs. (8) and (9) give us the frequency and angle (if it exists) at which the folds are located.

From Eq. (7), we obtain the point at which the folds coincide ($\phi_c = -\tau_{\text{eff}}/\sqrt{2}$) and that determines the cusp singularity.

From now on, we consider circularly polarized laser pulses $a_x = a_y$ and the main Compton line $n = 1$ (see Supplemental Material [29] for the results on linearly polarized laser pulses). We would like to find the optimal $\beta$ parameter for fixed $a_0$, $\tau$ for which the spectra would have the brightest maximum. Equation (9) shows that for narrowband and collimated emission, the cusp angle should lie close to the axis. Imposing an additional constraint $\theta_c = \pi$ on Eq. (9), we obtain an equation for $\beta_c$,

$$\beta_c \left( 1 + \frac{2a_0^2}{\sqrt{1 + \beta_c^2}} e^{-1/2} \right) = \sqrt{2} \tau a_0^2 e^{-1/2}, \quad (10)$$

where the exponential multiplier is due to the Gaussian temporal envelope and which could be solved either numerically or perturbatively for effectively large $a_0^2 \tau$: $\beta_c \simeq \sqrt{2e^{-1}} a_0^2 \tau - 2\sqrt{2} e^{-1} \frac{a_0^4 \tau}{\sqrt{1 + 2e^{-1} a_0^4 \tau^2}}$. This equation gives us the chirp value $\beta_c$ at which the cusp would lie on-axis. The corresponding frequency is given by $\omega_c = 1 - \frac{\sqrt{2} \beta_c}{\tau \sqrt{1 + \beta_c^2}}$.

One could notice that emission is *not* brightest exactly at the cusps. The values of the integral given by Eq. (4) near the cusp are determined by the Pearcey diffraction pattern. Thus, we do not have to demand that the cusp is on-axis, but rather that the maximum of the Pearcey pattern is located on-axis. Taylor-expanding the integral under the exponential in the amplitude $M$ around the cusp point $\phi_c$, we obtain the Pearcey integral Pe (see Supplemental Material [29]),

$$\frac{d^2 N_{ph}}{d\omega d\Omega}\Big|_{\theta = \pi} \approx \alpha \frac{\omega}{8\pi^2} \frac{a_0^2 e^{-1/4}}{\sqrt{1 + \beta^2}} \left( \frac{6\sqrt{2} \tau_{\text{eff}}^3}{\omega a_{\text{eff}}^2} \right)^{1/2} |\text{Pe}(x, y)|^2, \quad (11)$$

where $x, y$ are functions of $\omega, \beta$. Knowing the values $x_*, y_* \approx -2.16, 0$ at which $|\text{Pe}(x, y)|$ achieves its maximum, we obtain two equations $x(\omega, \beta) = x_*$, $y(\omega, \beta) = y_*$ which gives us the optimal $(\omega_*, \beta_*)$ pair found by analyzing the maximum of the Pearcey integral.

It turns out that even with the Pearcey maximum, the optimal chirp parameter is not found because the prefactor $B$ also depends on $\omega, \beta$ that could not be neglected in our case due to their variation in the region of interest [see Eq. (11)]: $\frac{d^2 N_{ph}}{d\omega d\Omega} \sim \sqrt{\omega(1 + \beta^2)} |\text{Pe}(x, y)|^2$. To improve our theoretical prediction of optimal chirp, we Taylor-expanded this expression around the Pearcey maximum $(\omega_*, \beta_*)$ up to the second order assuming that the actual optimal pair lies close to the Pearcey pair (see Supplemental Material [29]) and obtain corrected optimal values $(\omega_T, \beta_T)$. In the text, we would call this procedure "Taylor prefactor correction."

Figure 1 illustrates how varying the linear chirp parameter $\beta$ affects the incident laser pulse and, subsequently, the emission spectrum. When the chirp is increased, two effects come into play. On the one hand, stronger chirping produces
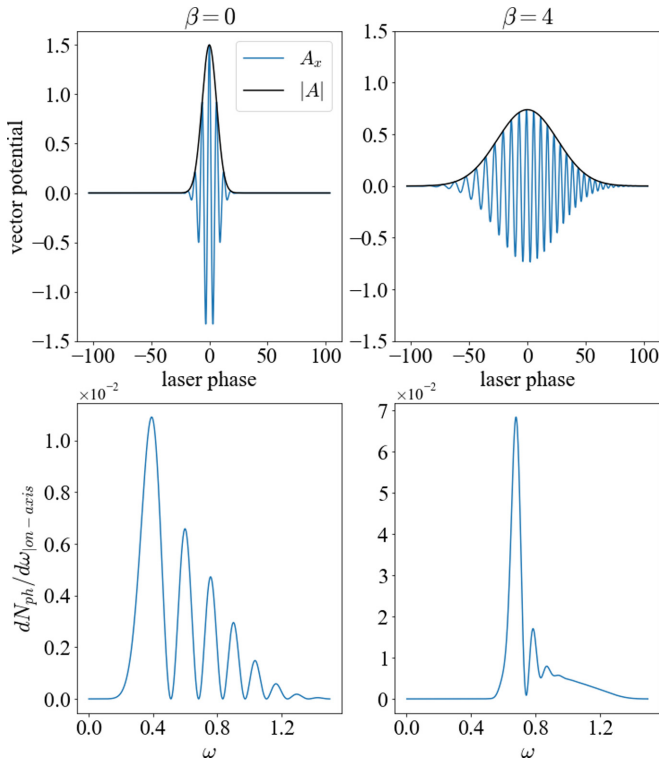
FIG. 1. Top: Vector potential of a linearly chirped laser pulse ($a_0 = 1.5$, $\tau = 2\pi$) for different chirp parameters $\beta = 0, 4$. Bottom: Corresponding backscattered spectra.

less intense and longer laser pulses for which the backscattered spectra are less broad and therefore more bright because the incident laser spectrum is constant. On the other hand, increasing the chirp moves the cusp point closer to the axis which, up to some point, also increases the peak spectrum value. For instance, we could see that changing $\beta$ from 0 to 4 in the laser pulse with $a_0 = 1.5$, $\tau = 2\pi$ leads to a narrower spectra with smaller number of subpeaks and a weak pedestal is created. For large $\beta$, the cusp point vanishes and increasing $\beta$ even further leads to a larger spectral pedestal along with a smaller spectral peak until it reaches the $\beta \gg 1$ limit.

Let us illustrate what the folds and cusp look like in our problem setting. Figure 2 shows backscattered spectra from a laser pulse ($a_0 = 2$, $\tau = 4\pi$) for different $\beta$ parameters. Due to the dependence of the laser amplitude and duration on chirp, the folds' profile significantly differs from the original article [20]. For larger laser intensities and duration, the maximal peak moves to higher frequencies and chirps and enters the region where the emission frequency is almost constant. That is why even Pearcey approximation (when we do not take into account the prefactor that depends on $\omega, \beta$) gives satisfactory results.

To obtain numerical data, we fixed the laser pulse amplitude and duration ($a_0, \tau$) and calculated the results on a linear grid over $\beta$ parameters. The numerical optimal $\beta$ value corresponds to the maximal photon peak observed from the simulation results on the grid. Figure 3 shows the color map for the normalized peak of the differential number of emitted photons as a function of ($a_0, \beta$) for $\tau = 4\pi$. We could see that
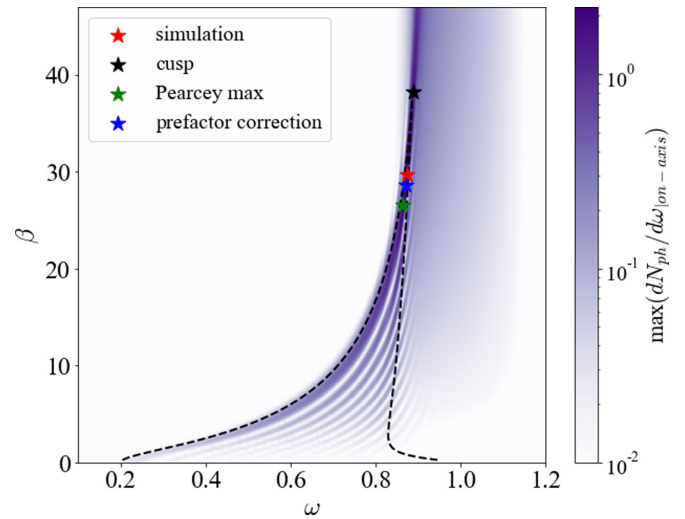


FIG. 2. Backscattered spectra for different $\beta$ parameters and $a_0 = 2$, $\tau = 4\pi$. The dashed black line shows folds terminating at the cusp (black star). The red star shows the maximal peak found from simulations; green and blue stars show the location of the maximal peak obtained from different analytical methods.
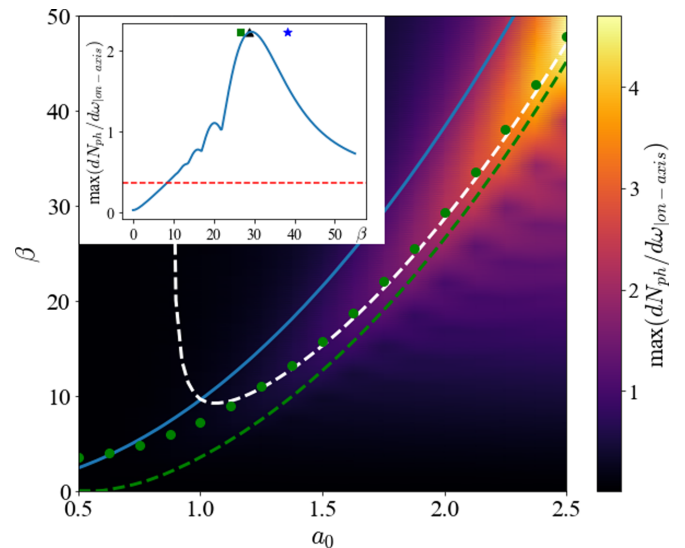


FIG. 3. Peak of the differential number of emitted photons (color map) as a function of laser amplitude $a_0$ and chirp parameter $\beta$ for $\tau = 4\pi$. The green dots show the optimal $\beta$ at which the peak has the highest value for a fixed $a_0$, the solid blue line shows $\beta$ as a function of $a_0$ obtained by solving the system of cusp-on-axis equations, the dashed green line shows optimal $\beta(a_0)$ obtained by Pearcey approximation of the scattering integral, while the white dashed line shows $\beta(a_0)$ obtained by the Taylor prefactor correction procedure to the Pearcey approximation. One could see that from $a_0 > 1$, there is a very good agreement between the Taylor prefactor correction and actual numerical optima. Inset: Slice of the color map at $a_0 = 2$; the black triangle stands for the prediction of optimal $\beta$ from the Taylor procedure (blue and green symbols stand for the cusp-on-axis and Pearcey prediction, respectively), and the red dashed line shows the limit $\beta \gg 1$ for the given $a_0, \tau$.
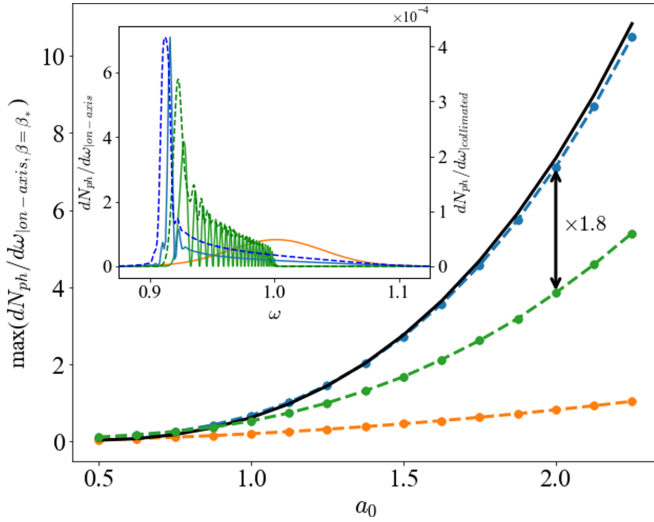
FIG. 4. Peak of the differential number of emitted photons estimated at optimal chirp value $\beta_*$ as a function of $a_0$ for $\tau = 6\pi$. The blue line shows the peak values estimated from numerical simulations, the black solid line shows the analytical prediction from the Pearcey approximation, the green line shows the peak of the unchirped spectra for $a_{\text{eff}}$, $\tau_{\text{eff}}$ estimated at optimal chirp value $\beta_*$, and the orange line shows the linear Compton limit for $\beta \gg 1$. For example, for $a_0 = 2$, there is an almost double enhancement in the peak value compared to the nonchirped case, and over eight time enhancement compared to the limit case $\beta \gg 1$. Inset: $a_0 = 2$. The solid lines show on-axis spectra (left $y$ axis): blue shows the optimally chirped case, green shows the unchirped nonlinear Compton spectra for $a_{\text{eff}}$, $\tau_{\text{eff}}$ estimated at optimal chirp value $\beta_*$, and orange shows the linear Compton limit case for $a_0$, $\tau$. The blue and green dashed lines (right $y$ axis) show the optimally chirped spectra and nonlinear Compton spectra collimated over $\theta_c = 0.1/\gamma$.

for a fixed $a_0$, there is the optimal $\beta$ value (which is greater for larger $a_0$, $\tau$) at which the photon peak is maximal. Our goal is to analytically estimate this optimal value. One could see that solving the system of cusp-on-axis equations overshoots the target value and the agreement is generally not very good. With the Pearcey approximation, the analytical prediction is much better for larger $a_0$ but still not good enough. Finally, the Taylor prefactor correction procedure gives a very satisfactory analytical prediction. The same could be seen on the inset slice. Similar results were found for different laser pulse durations (for $\tau = 2\pi$, $6\pi$, see Supplemental Material [29]), although for larger duration the analytical prediction starts to work from less intense values of $a_0$.

To demonstrate the benefit of using chirped laser pulses, we compared the peak photon spectrum values with the unchirped case. Figure 4 illustrates that using optimally chirped laser pulses increases the peak of the differential number of emitted photons compared to the unchirped nonlinear Compton spectrum (for $a_{\text{eff}}$, $\tau_{\text{eff}}$ evaluated at optimal chirp value $\beta_*$) and limit case for $\beta \gg 1$. For larger $a_0$, the enhancement is more noticeable. On the inset figure, we could see that the optimally chirped spectra has a narrow and bright single peak on top of a weaker pedestal, while the unchirped nonlinear Compton spectrum presents a typical broadband interference substructure. After collimation over a small angle $\theta_c = 0.1/\gamma$, the spectrum remains narrow, but for larger collimation angles, it would be significantly broader. It would be interesting to have a look at real values corresponding to a found optimally chirped laser pulse. For example, for $a_0 = 2$, $\tau = 6\pi$, the optimal chirp $\beta_{opt} \approx 48$. For a laser with $\omega_0 = 1.55$ eV, the duration would be $\tilde{\tau} = 8$ fs (bandwidth $\sim 1/\tau \approx 0.05$) and group delay dispersion (GDD) $\beta^{(2)} = \beta_{opt}\tilde{\tau}^2 \approx 3072$ fs$^2$.

In this Letter, we considered the case of a laser pulse chirped in the spectral domain. In the temporal domain, the amplitude and duration of such laser pulse depend on the chirp parameter. We showed that there is an optimal chirp at which the backscattered spectrum has the brightest photon peak which results from the interplay of two effects. First, when we increase chirp, the laser energy remains constant while the backscattered spectrum is shrunk towards $\omega \sim 1$, which increases the maximal peak. Second, larger chirp leads to the cusp moving closer to the axis, which makes the spectra brighter as well until the cusp goes too far and the spectral peak begins to fall down. Also, we discussed the analytical approach (and some improvements to it) to predict the optimal chirp value and showed that for relatively large laser amplitudes and laser duration, the given approach works very well and one does not need to perform costly linear scans to find the values of interest. Also, chirping the laser pulse gives a significant improvement over an unchirped case in terms of the spectrum narrowness and brightness. Finally, these results could help to move closer towards the experimental realization.

The code to reproduce the results from the Letter can be found in [30].

[1] T. S. Carman, V. Litveninko, J. Madey, C. Neuman, B. Norum, P. G. O'Shea, N. R. Roberson, C. Y. Scarlett, E. Schreiber, and H. R. Weller, Nucl. Instrum. Methods Phys. Res., Sect. A **378**, 1 (1996).

[2] W. Bertozzi, J. A. Caggiano, W. K. Hensley, M. S. Johnson, S. E. Korbly, R. J. Ledoux, D. P. McNabb, E. B. Norman, W. H. Park, and G. A. Warren, Phys. Rev. C **78**, 041601(R) (2008).

[3] F. Albert, S. Anderson, D. Gibson, C. Hagmann, M. Johnson, M. Messerly, V. Semenov, M. Shverdin, B. Rusnak, A. Tremaine *et al.*, Phys. Rev. Spec. Top.-Accel. Beams **13**, 070704 (2010).

[4] F. Albert, S. Anderson, D. Gibson, R. Marsh, S. Wu, C. Siders, C. Barty, and F. Hartemann, Phys. Rev. Spec. Top.-Accel. Beams **14**, 050703 (2011).

[5] B. J. Quiter, B. A. Ludewigt, V. V. Mozin, C. Wilson, and S. Korbly, Nucl. Instrum. Methods Phys. Res., Sect. B **269**, 1130 (2011).

[6] C. G. Geddes, S. Rykovanov, N. H. Matlis, S. Steinke, J.-L. Vay, E. H. Esarey, B. Ludewigt, K. Nakamura, B. J. Quiter, C. B. Schroeder *et al.*, Nucl. Instrum. Methods Phys. Res., Sect. B **350**, 116 (2015).

[7] J. Faure, Y. Glinec, A. Pukhov, S. Kiselev, S. Gordienko, E. Lefebvre, J.-P. Rousseau, F. Burgy, and V. Malka, Nature (London) **431**, 541 (2004).

[8] I. Blumenfeld, C. E. Clayton, F.-J. Decker, M. J. Hogan, C. Huang, R. Ischebeck, R. Iverson, C. Joshi, T. Katsouleas, N. Kirby *et al.*, Nature (London) **445**, 741 (2007).

[9] V. G. Nedorezov, A. A. Turinge, and Y. M. Shatunov, UFN **174**, 353 (2004).

[10] S. Rykovanov, C. Geddes, J. Vay, C. Schroeder, E. Esarey, and W. Leemans, J. Phys. B: At., Mol. Opt. Phys. **47**, 234013 (2014).

[11] V. G. Nedorezov, S. G. Rykovanov, and A. B. Savel'ev-Trofimov, Phys. Usp. **64**, 1214 (2021).

[12] F. V. Hartemann, A. L. Troha, N. C. Luhmann, Jr., and Z. Toffano, Phys. Rev. E **54**, 2956 (1996).

[13] F. V. Hartemann and S. S. Q. Wu, Phys. Rev. Lett. **111**, 044801 (2013).

[14] S. G. Rykovanov, C. G. R. Geddes, C. B. Schroeder, E. Esarey, and W. P. Leemans, Phys. Rev. Accel. Beams **19**, 030701 (2016).

[15] T. Heinzl, D. Seipt, and B. Kämpfer, Phys. Rev. A **81**, 022125 (2010).

[16] D. Seipt and B. Kämpfer, Phys. Rev. A **83**, 022101 (2011).

[17] B. Terzić, K. Deitrick, A. S. Hofler, and G. A. Krafft, Phys. Rev. Lett. **112**, 074801 (2014).

[18] I. Ghebregziabher, B. A. Shadwick, and D. Umstadter, Phys. Rev. Spec. Top.-Accel. Beams **16**, 030705 (2013).

[19] D. Seipt, S. G. Rykovanov, A. Surzhykov, and S. Fritzsche, Phys. Rev. A **91**, 033402 (2015).

[20] V. Y. Kharin, D. Seipt, and S. G. Rykovanov, Phys. Rev. Lett. **120**, 044802 (2018).

[21] D. Seipt, V. Y. Kharin, and S. G. Rykovanov, Phys. Rev. Lett. **122**, 204802 (2019).

[22] E. Johnson, E. Breen, G. A. Krafft, and B. Terzić, Phys. Rev. Accel. Beams **25**, 054401 (2022).

[23] M. A. Valialshchikov, V. Y. Kharin, and S. G. Rykovanov, Phys. Rev. Lett. **126**, 194801 (2021).

[24] M. Valialshchikov, V. Y. Kharin, and S. G. Rykovanov, Quantum Electron. **51**, 812 (2021).

[25] A. Debus, M. Bussmann, M. Siebold, A. Jochmann, U. Schramm, T. Cowan, and R. Sauerbrey, Appl. Phys. B **100**, 61 (2010).

[26] A. Jochmann, A. Irman, M. Bussmann, J. P. Couperus, T. E. Cowan, A. D. Debus, M. Kuntzsch, K. W. D. Ledingham, U. Lehnert, R. Sauerbrey, H. P. Schlenvoigt, D. Seipt, T. Stohlker, D. B. Thorn, S. Trotsenko, A. Wagner, and U. Schramm, Phys. Rev. Lett. **111**, 114803 (2013).

[27] Q. Z. Lv, E. Raicher, C. H. Keitel, and K. Z. Hatsagortsyan, Phys. Rev. Lett. **128**, 024801 (2022).

[28] J. D. Jackson, *Classical Electrodynamics*, 3rd ed. (Wiley, New York, 1998).

[29] See Supplemental Material at http://link.aps.org/supplemental/10.1103/PhysRevA.106.L031501 for details of the Pearcey approximation and Taylor prefactor correction procedures, additional figures for incident laser pulses of different lengths and intensities, results of linearly polarized incident laser pulses, and alternative numerical optimization technique.

[30] https://github.com/maxbalrog/optimal-chirp.

[31] https://rscf.ru/project/22-22-01031/.